ELSEVIER

Journal of Power Sources 112 (2002) 273–289

JOURNAL OF POWER SOURCES

www.elsevier.com/locate/jpowsour

Carbon dioxide separation from high temperature fuel cell power plants

Stefano Campanari

Department of Energetics, Politecnico di Milano, Piazza Leonardo da Vinci 32, 20133 Milan, Italy

Received 24 January 2002; accepted 17 July 2002

Abstract

High temperature fuel cell technologies, solid oxide fuel cells (SOFCs) and molten carbonate fuel cells (MCFCs), are considered for their potential application to carbon dioxide emission control. Both technologies feature electrochemical oxidisation of natural gas reformed fuels, avoiding the mixture of air and fuel flows and dilution with nitrogen and oxygen of the oxidised products; a preliminary analysis shows how the different mechanism of ion transport attributes each technology a specific advantage for the application to CO_2 separation. The paper then compares in the first part the most promising cycle configurations based on high efficiency integrated SOFC/gas turbine ''hybrid'' cycles, where CO_2 is separated with absorption systems or with the eventual adoption of a second SOFC module acting as an ''afterburner''. The second part of the paper discusses how a MCFC plant could be ''retrofitted'' to a conventional fossil-fuel power station, giving the possibility of draining the majority of CO_2 from the stack exhaust while keeping the overall cycle electrical efficiency approximately unchanged.

Keywords: SOFC; MCFC; CO_2 separation; Power plants

1. Introduction

A rapidly growing issue in the field of power generation is CO_2 emissions reduction for greenhouse effect control. As long as fossil fuels are used for power generation, one of the major option for CO_2 emission control is the capture of the CO_2 generated by the fuel oxidisation, and its subsequent disposal to an appropriate site for permanent storage.

This work concentrates on the great potential of the high temperature fuel cells technology for the application to carbon dioxide separation. One of the distinctive features of the high temperature fuel cell technology is the oxidisation of fuels like natural gas with an internal reforming process which involves the transportation of ions through the electrolyte from the air flow (cathode flow) to the fuel flow (anode flow), avoiding the complete mixture of the two flows and the dilution with nitrogen and oxygen of the oxidised components.

A preliminary comparison of the SOFCs and MCFCs technologies shows how their different features may then ensure specific advantages and/or disadvantages when applied to carbon dioxide separation. The work then focuses in the first section on the particular advantages of SOFCs and presents an assessment of their potential for the application to medium or large scale power plants, fuelled with natural gas and based on the SOFC/gas turbine ''hybrid'' cycle concept. Interest and feasibility of these technologies is demonstrated by the Rolls-Royce and Siemens–Westinghouse projects for multi-MW hybrid cycles [1] as well by the Shell demonstration project of a double SOFC for CO_2 capture power plant (scheduled for 2003 in Norway), intended as a milestone for the future development of 15–50 MW power plants where the separated CO_2 should be used for ''enhanced oil recovery'' by injection in oil wells [2].

Different cases are investigated, where the power contribution and the cell voltage of the additional SOFC ranges from zero up to a calculated value. The alternative option of oxygen combustion of the fuel cell anode exhaust, and the matter of the incondensable species contained in natural gas, has been addressed. In spite of low efficiency decay versus similar cycles without CO_2 removal, these plants show the potential to approach 70% LHV electric efficiency with 90% CO_2 abatement.

The last section of the paper discusses how MCFCs can be applied to CO_2 separation, highlighting the possibility of

Abbreviations: LHV, fuel lower heating value; MCFC, molten carbonate fuel cell; SOFC, solid oxide fuel cell; USC, ultra super critical

E-mail address: stefano.campanari@polimi.it (S. Campanari).

0378-7753/02/$ – see front matter
PII: S0378-7753(02)00395-6

Nomenclature

F	Faraday's constant (96,439 C/mol)
m	mass flow (kg/s)
p	pressure (bar)
ΔS	entropy loss (J/kg K)
T	temperature (K or °C)
U_a	air utilisation factor ($m_{oxygen,consumed}/m_{oxygen,in}$)
U_f	fuel utilisation factor ($m_{fuel,consumed}/m_{fuel,in}$)
V_c	cell voltage
ΔV	voltage difference (Eq. (A.1))
W_{el}	electric work (J/kg)
W_{rev}	reversible work (J/kg)
X_{CH_4}	methane contribute to hydrogen formation
X_{CO}	carbon monoxide contribute to hydrogen formation

Greek symbols

η_{el}	electrical efficiency (Eq. (A.2))
Γ_{H_2}	fuel equivalent hydrogen content (Eq. (A.3))

Subscripts

amb	ambient
f	fuel
ref	reference conditions

"retrofitting" existing fossil-fuel power plants by extracting CO_2 from their stack exhausts. When applied to modern supercritical coal steam plants, this technology could keep almost unchanged the plant electrical efficiency while adding 40% power output and separating more than 70% of the CO_2 otherwise vented.

Even if the present development status of high temperature fuel cells (still characterised by high costs and small-scale demonstrations) suggests that their application to large scale power plants is probably confined in a medium-term perspective, the great potential of this technology in CO_2 emissions control may ensure it a relevant role in the next future power generation.

2. Comparison between MCFC and SOFC for the application to CO_2 separation

2.1. Basic principles

High temperature fuel cells feature hydrocarbon fuel oxidisation based on an internal reforming process involving different mechanisms for ion transportation across the cell electrolyte. As a result SOFC and MCFC operation features different flow arrangement and specific chemical processes (Fig. 1).

- In SOFCs, only oxygen ions are transported by the electrolyte, with the following cell reactions:

$$\begin{cases} H_2 + O^{2-} \rightarrow H_2O + 2e^- & \text{(anode)} \\ \frac{1}{2}O_2 + 2e^- \rightarrow O^{2-} & \text{(cathode)} \end{cases} \quad (1)$$

  where hydrogen is generated from the fuel (natural gas) by steam reforming and CO-shift reactions:

$$C_nH_m + nH_2O + \text{heat} \rightarrow (\tfrac{1}{2}m + n)H_2 + nCO \quad (2)$$

$$CO + H_2O \leftrightarrow H_2 + CO_2 + 44.48\,\text{MJ/kmol}_{CO} \quad (3)$$

  CO_2 is then completely contained by the cell anode exhaust flow, which is a variable proportion mixture of $CO + CO_2 + H_2 + H_2O$.
- In MCFCs, the cathode inlet flow shall contain both oxygen and CO_2: oxygen ions are transported across the electrolyte bounded to CO_2 in the form of carbonate ions (CO_3^{2-}), and CO_2 is contained both by anode exhaust flow (formed by oxidisation of the fuel and by the carbonate ions themselves) and by cathode exhaust flow (because the electrochemical reactions cannot consume

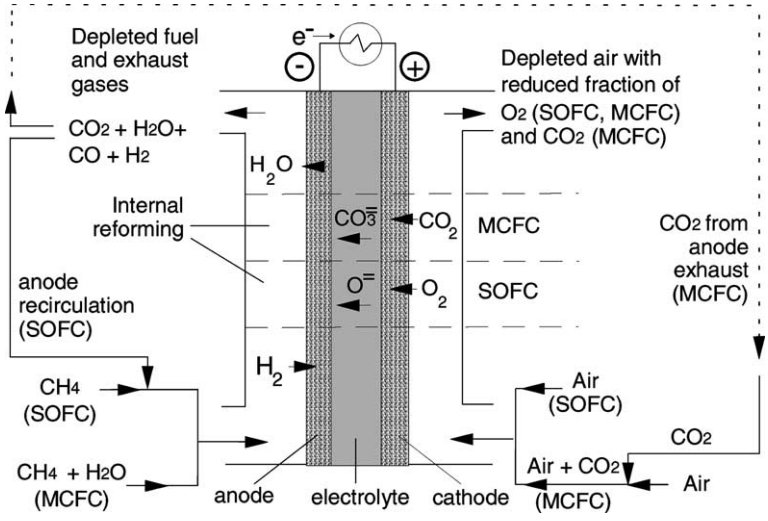

Fig. 1. MCFC and SOFC conceptual scheme.

Table 1
Inlet and outlet flow composition for the MCFC and SOFC plants of Fig. 2

Composition (mol%)	Fuel cell	CO	H_2	CH_4	C_xH_y	CO_2	O_2	H_2O	N_2	Ar	Outlet flows (kg/kg_{fuel})	CO_2 mass percentage
(1) Anode inlet	MCFC	0	0	36.3	1.8	0	0	60.2	1.7	0	–	–
	SOFC	6.5	20.6	13.5	0	22.4	0	35.2	2.0	0	–	–
(2) Anode outlet	MCFC	5.2	6.1	0	0	48.7	0	39.4	0.6	0	13.4	78.5
	SOFC	7.5	12.1	0	0	25.9	0	53.1	1.40	0	4.14	100
(3) Cathode inlet	MCFC		0			18.2	12.3	15.9	52.9	0.65	–	–
	SOFC		0			0	20.7	1.03	77.3	0.92	–	–
(4) Cathode outlet	MCFC		0			5.65	6.85	20.2	66.6	0.80	28.3	21.5
	SOFC		0			0	15.5	1.10	82.4	0.98	42.3	0

the totality of CO_2 fed to the cathode). This behaviour is synthesised by the MCFC global reactions (together with Eqs. (2) and (3)):

$$\begin{cases} H_2 + CO_3^{2-} \rightarrow H_2O + CO_2 + 2e^- & \text{(anode)} \\ \frac{1}{2}O_2 + CO_2 + 2e^- \rightarrow CO_3^{2-} & \text{(cathode)} \end{cases} \quad (4)$$

Cell cathode is generally fed by recycling a substantial fraction of CO_2 from the anode exhaust, as shown in the conceptual scheme of Fig. 1.

2.2. Application to CO_2 separation

Further features emerge when comparing SOFC and MCFC typical inlet and outlet flow compositions, which are listed in Table 1 based on the plant configurations shown in Fig. 2. The two plant configurations are based on recently demonstrated technologies.

- SOFC makes reference to the Siemens–Westinghouse tubular technology experimented in a 100 kW atmospheric power plant at Arnhem, The Netherlands [3,4].
- MCFC plant is based on the fuel cell energy "direct fuel cell" technology as by the early simulations of EPRI [5] and by the 2.5 MW experimental power plant of St. Clara, CA, USA [6].

In both the cases, mass flows have been normalised to an air flow input of 1.0 kg/s; SOFC utilisation factors have been set to 30% (air, i.e. 3.3 stoichiometric) and 85% (fuel, including recycling). Gas compositions are calculated based

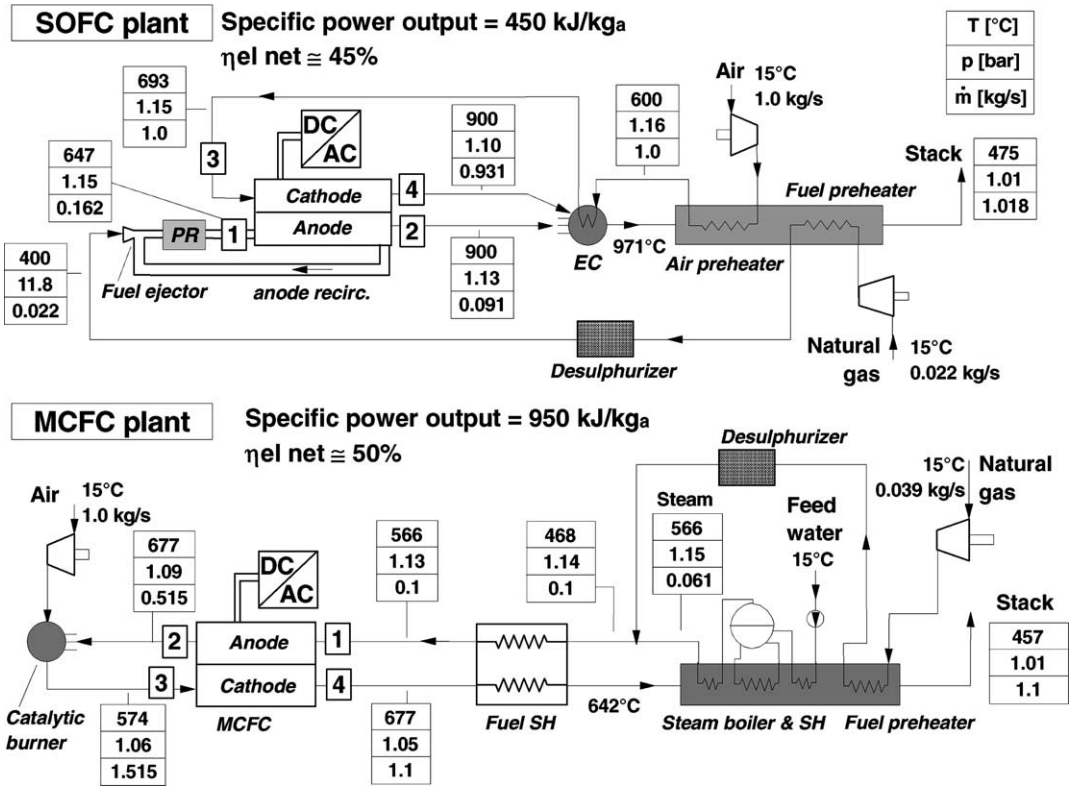

Fig. 2. Operating conditions of a MCFC and of a SOFC plant (PR: pre-reforming chamber; EC: exhaust residual combustion; see also Fig. 3).

on a fuel cell simulation model addressed together with other relevant assumptions in Appendix A and in [7,8].

The SOFC concentrates all the CO_2 production in the anode exhaust flow, where for each kilogram per second of fresh fuel it generates 4.14 kg/s of oxidised fuel with a 25.9% molar fraction (48.4% mass) of carbon dioxide. It is then possible to make available the anodic exhaust flow for a CO_2 separation train, avoiding the exhaust residual combustion (indicated with EC in Fig. 2), which normally takes place mixing the cathode exhaust and the anode exhaust flow. The high concentration of CO_2, which is not mixed with nitrogen and excess oxygen coming from air, makes particularly low the energetic loss for CO_2 separation. This approach will be considered in detail in the first part of the paper.

The MCFC requires the presence of CO_2 both in the anode and in the cathode flow. The majority of CO_2 exiting the fuel cell (78.5%) is concentrated in the anode exhaust, but this flow has to be recycled (totally or in a major fraction) to the cathode in order to sustain the formation of carbonate ions transported by the electrolyte (Eq. (4)).

The necessity of a substantial anodic exhaust recycling prevents the possibility of easily separating carbon dioxide from a CO_2-rich flow, leaving this opportunity to SOFCs only: the MCFC plant global CO_2 production is ultimately contained by the cathode outlet flow (#4 in Fig. 2), where CO_2 is mixed with nitrogen and excess oxygen coming from the catalytic burner, thus generating a larger mass flow rate stream (28.3 kg/s for each kilogram per second of fresh fuel), with low CO_2 concentration (5.7 mol%, 9.2% mass).

The peculiarity of the mechanism of CO_2 transport across the MCFC may turn into an advantage if the MCFC cathode is fed with exhaust gases generated by a separated power plant, which could already contain the requested CO_2 without needing any exhaust recycling. The MCFC could be placed downstream to a conventional ‘‘combustion fired’’ power plant with the aim of concentrating and then separating a fraction of the CO_2 otherwise vented. This approach is considered in detail in the second part of the paper.

3. CO_2 separation from high efficiency SOFC/gas turbine power plants

As discussed above, it is possible to exploit the high CO_2 concentration at SOFC anode outlet to set up a plant arrangement destined to CO_2 capture. This approach can be applied with particularly bright results if the SOFC is integrated in a high efficiency plant based on a gas turbine cycle.

The integration of SOFCs with gas turbine cycles has been investigated in the last years both for small-scale applications and for large size electric energy generation [9,10]. The extremely high potential of this novel technology, recently demonstrated in a small-scale ‘‘hybrid’’ plant [11,12], can be synthesised in the possibility of exceeding combined cycles performances with the further advantage of yielding extremely low emissions. This promising SOFC technology is considered here for its great potential for the application to the CO_2 emission control.

After the discussion of some preliminary modelling assumptions, different cycle configurations are investigated in the following, based on intercooled and recuperated hybrid cycles. Detailed results are presented, both in terms of first and second law analysis, together with the thermodynamic properties of the most relevant points, and the cycle operating parameters.

3.1. Stack modification for the application to CO_2 separation

The SOFC stack standard (or most common) configuration of Fig. 2 generates a single outlet stream: cathode and anode exhausts (spent air and spent fuel) react burning in a combustion plenum. The generated exhaust gases are then used to preheat the inlet airflow. This configuration is shown with greater detail on the left side of Fig. 3 for a tubular SOFC module.

The alternative discussed here requires the adoption of a gas seal to keep the cathode and anode exhaust gases separated, thus introducing a modification to the original ‘‘seal-less tube’’ SOFC configuration. This modification has been already proposed by Shell and Siemens–Westinghouse [17] for the application to the third plant scheme discussed in the following. The resulting SOFC stack is shown on the right side of Fig. 3. SOFC operating conditions throughout the proposed cycles are maintained as discussed in Appendix A, with the SOFC schematically represented as a box with two inlet streams (fuel and oxidiser) and two outlet streams (oxidised fuel and depleted oxidiser).

3.2. Gas turbine cycle and CO_2 separation model

The fuel cell model addressed in Appendix A is integrated in a more general gas turbine and steam cycle calculation code, which has been extensively used for accurate performance evaluations of low CO_2 emissions gas turbine based complex cycles [18,19]. The modular structure of this computer code allows the analysis of any power cycle described by a network of components chosen among a list of 16 types, including compressor, combustor, turbine, heat exchanger, heat recovery steam cycle, oxygen plant, saturator, fuel cell.

CO_2 chemical absorption process has been evaluated with a commercial software [20] while performance of the physical absorption process has been calculated by the same procedure illustrated in [21]. In the latter case, absorption pressure has been set to achieve the given 90% CO_2 removal. The main assumptions adopted for the calculation of the plants are summarised in Table 2.

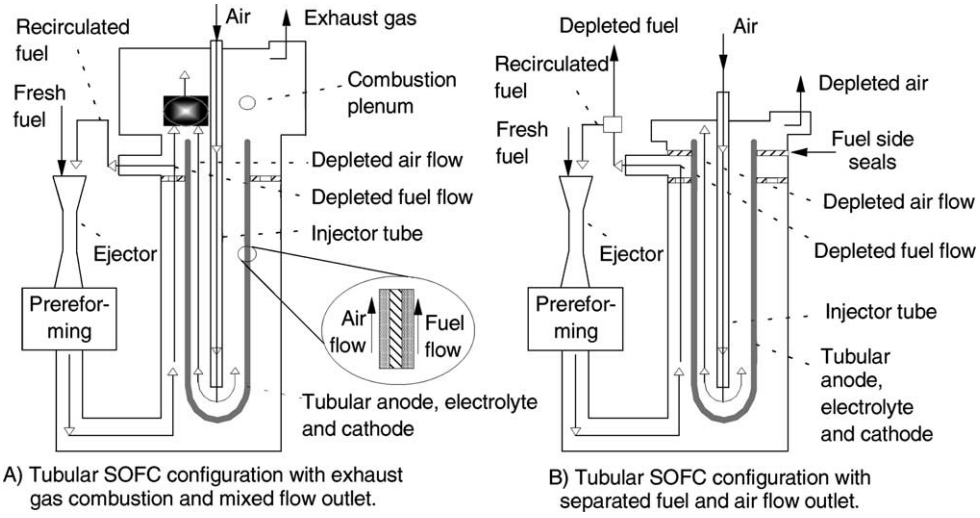

Fig. 3. Tubular SOFC stack: (A) standard configuration and (B) alternative configuration.

3.3. Cycles configurations

Exploiting the SOFC features, different cycle configurations are discussed, based on intercooled and recuperated ‘‘hybrid’’ gas turbine cycles integrated with the SOFC system.

The plant size has been set in all cases according to a natural gas input of 100 MW (LHV), thus referencing to possible future application of this technology to medium-scale power plants with net electrical power output in the range of 60–70 MW, a size coherent with the possibility of a substantial CO_2 consumption for enhanced oil recovery by injection in oil wells [2,17].

The gas cycle configuration required by these plants is anyway very different from the usual practice: turbomachinery feature unconventional pressure ratios and turbine inlet temperatures, so that they should be designed ad hoc for the application to these plants. A partial counterpart to this unfavourable aspects has been given by the adoption of uncooled turbines, even if higher firing temperatures, coupled to higher pressure ratios, could generally lead to a slightly better performance.

The fuel cell acts as the primary fuel oxidiser, and each kind of configuration feature a different approach to the separation of CO_2 from the fuel cell anode exhaust (spent fuel) flow.

Two CO_2 removal ‘‘strategies’’ have been investigated and discussed below.

Table 2
Main assumptions adopted for the calculation of the plants

Compressor polytropic efficiency	0.90
Turbine polytropic efficiency	0.92
Maximum turbine inlet temperature (°C)	900
Minimum ΔT in recuperators (°C)	30
$\Delta p/p$ heat exchangers	2%
Physical absorption minimum flash drum pressure (bar)	1.05

3.3.1. Separation strategy 1: CO_2 removal train

The first strategy (Fig. 4) is based on the addition of a fuel processing section to the power plant, where a CO_2 separation train extracts carbon dioxide from the cell anode exhausts. This approach has also been considered in a previous paper [22] and is completed here by a second law analysis.

Two very similar plant configurations are proposed, which rely on a different concept to achieve the desired CO_2 sequestration.

A) In the first option, the SOFC anode exhaust gas is shifted to a $CO_2 + H_2O + H_2$ mixture, subsequently cooled for water condensation and pressurised for CO_2 and hydrogen separation by a physical absorption process; the recovered hydrogen can either be recycled in the fuel cell or burnt with air to increase gas turbine inlet temperature. The remaining CO_2 flow is sent to the liquefaction process (Fig. 4A). A detailed analysis of this option is presented in the following.

B) In the second option, the SOFC anode exhaust is cooled to extract the condensed water, and a large fraction of CO_2 is directly removed by chemical absorption, while the remaining $CO + H_2$ mixture with a small fraction of CO_2 is recycled in the fuel cell. In order to carry out absorption at about ambient temperature, syngas exiting the anode side is cooled at first through an expansion to near atmospheric pressure, by preheating syngas deprived of CO_2 and finally by producing low pressure steam. Syngas is then cooled down to 35 °C to further condense the residual steam fraction and submitted to the absorber where a countercurrent flow of aqueous solution of diethanolamine (DEA) captures about 99% of the present CO_2 (Fig. 4B).

After absorption and preheating, a hydrogen and CO-rich syngas deprived of CO_2 is ready to be recycled to the fuel cell. In order to avoid setting up a fully closed loop, which

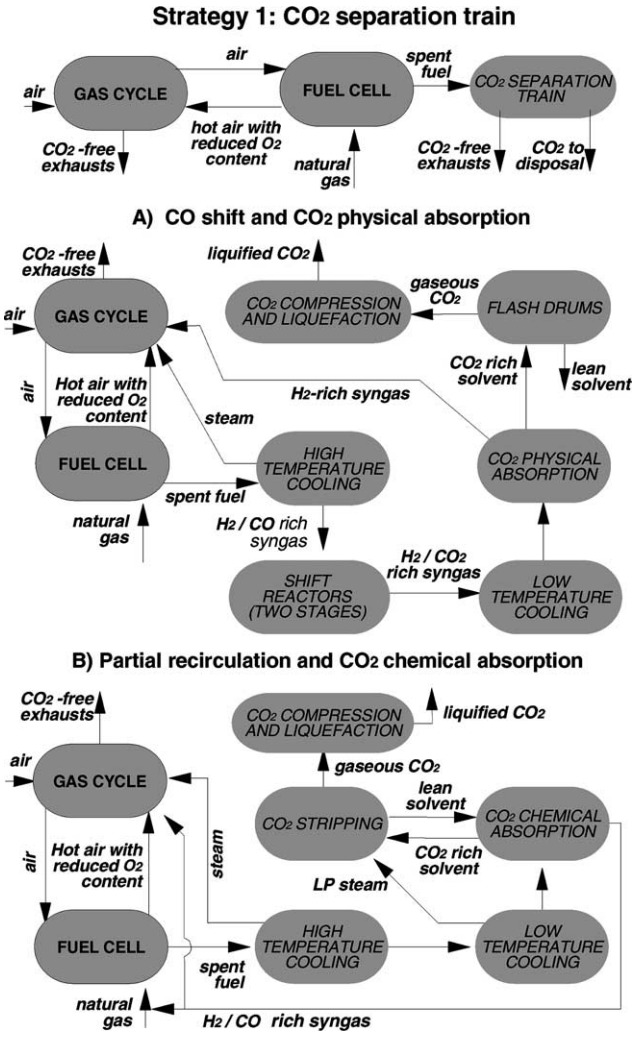

Fig. 4. Conceptual overview of the power cycles with CO_2 separation train from the SOFC anode exhaust.

would tend to accumulate inert species (e.g. nitrogen contained in the natural gas), a fraction of syngas flow is burned in a re-heat combustor of the gas turbine cycle, properly balancing the power output gain of the gas turbine (due to the increased turbine inlet temperature) with the increased CO_2 emission (due to the high CO content of the syngas). Other details on this plant configuration can be found in [22].

Both plants are designed to achieve 90% CO_2 removal, and approach 70% LHV efficiency. About 5% power output comes from the turboexpander which cools the cell depleted fuel. SOFC operates with the parameters of Table 9 in Appendix A.

The most representative option, despite its slightly higher complexity, is probably the first; results of its detailed simulation are shown in Fig. 5 and Table 3. This option is actually advantaged by:

1) more favourable gas turbine/SOFC power output ratio (0.29 versus 0.20), which could enhance the plant economics considered that fuel cells are expected to have a specific cost considerably higher than gas turbines [23];
2) lower consumption for auxiliaries (5.5 versus 8.2% of the net output, mostly due to the reduction of the power required to compress the syngas before CO_2 absorption) and a lower heat released to cooling fluids;
3) simpler physical absorption process, thanks to higher CO_2 mass flow rate in the syngas.

The distinguishing part of the fuel processing section is the substantial conversion to CO_2 of CO contained in the flow at anode side exit, which is easily accomplished through the shift reaction (Eq. (2)).

The abundance of steam in the mixture exiting the fuel cell anode (H_2O/CO ratio is 5.63) allows converting almost all the CO, ''relocating'' most of the fuel heating value to hydrogen.

According to the most usual technology practice, the shift reaction process is divided in two steps carried out at about 350 and 200 °C, respectively, depending on the different catalysts employed.

The conditioned syngas is then cooled and pressurised for CO_2 removal. The flow exiting at the top of the absorber is preheated and finally burnt in the gas cycle. In correspondence of a gas cycle pressure ratio of 3.8:1, its heating value is enough to raise the turbine inlet temperature up to 900 °C (maximum value admitted without blade cooling). Another possibility would be to partially recycle hydrogen, balancing the cycle nitrogen flow and enhancing the overall SOFC fuel oxidisation. This option has the disadvantages of: (i) lowering the GT power output; and (ii) requiring a higher SOFC air utilisation factor and a higher duty on the SOFC internal air preheating. The first option has been selected here because of its more equilibrated power distribution (2.8:1 for SOFC versus GT and syngas expander) and more conservative SOFC operating parameters.

3.3.2. Separation strategy 2: double-SOFC electrochemical CO_2 concentration

The next proposed configuration (Fig. 6) simulates the adoption of a second SOFC module (''SOFC-2'') which has the function of approaching a complete oxidisation of the spent fuel flow, thus acting as an ''afterburner'' and enhancing the CO_2 concentration of the anode exhaust gases. This concept has already been proposed in literature for stand-alone SOFCs in a future demonstration plant [2,17].

The plant scheme is shown in detail in Fig. 7. Compressed air is heated in sequence by a recuperator that recovers heat from gases after the turbine expansion, by two syngas coolers and by a high temperature heat exchanger. Air flowing to the cathode side is preheated at about 720 °C. A 10% fraction of compressed air shall be mixed with the SOFC cathode exhaust before feeding the SOFC-2 cathode inlet, in order to reduce the SOFC-2 operating temperatures, thus also slightly enhancing the oxygen fraction of SOFC-2 cathode inlet flow. Both syngas coolers have the function of preheating the first SOFC inlet air; the first syngas

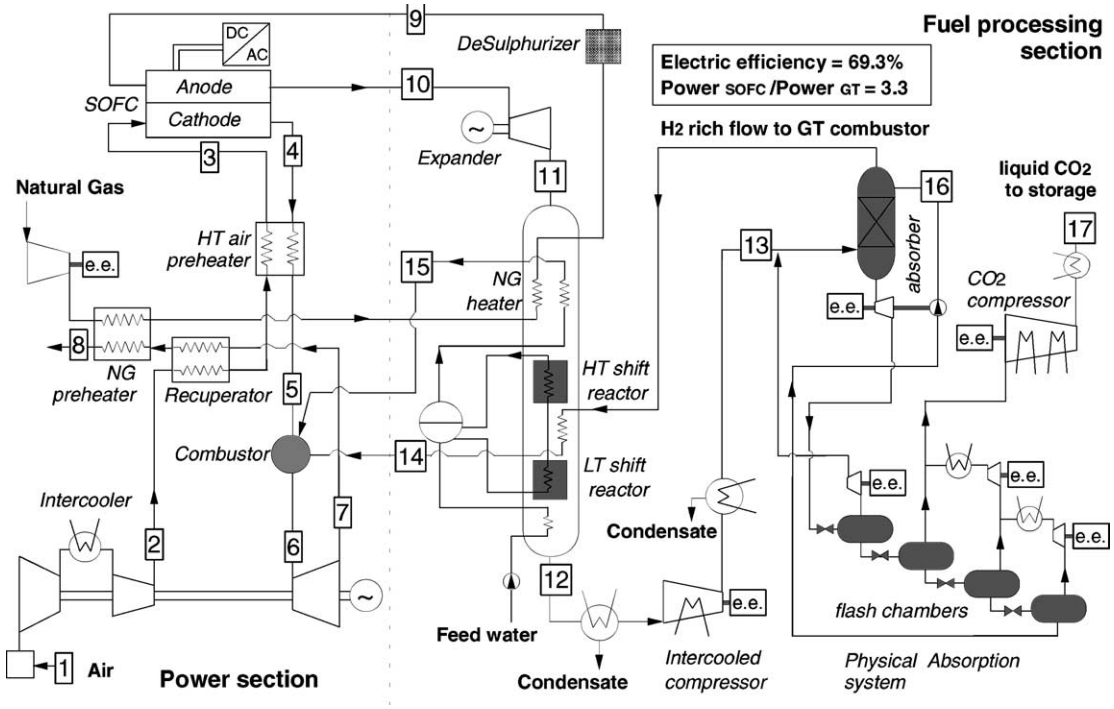

Fig. 5. Cycle configuration (Fig. 4A) with CO shift of cell anode exhaust and CO_2 physical absorption.

cooler avoids excessive temperatures at SOFC-2 anode inlet. Preheated fuel is fed to the anode side of the cell.

The first SOFC operates with the parameters of Table 9 in Appendix A. Since the first SOFC does not carry out a complete oxidisation of the fuel introduced (see composition in Table 4), the flow at the anode side exit contains relevant fractions of unconverted H_2 and CO mixed with CO_2 and steam. The second fuel cell works in this simulation with 90% fuel oxidisation, approaching a complete oxidisation of the spent fuel flow and generating an anode exhaust with about 33% CO_2, less than 2% of unreacted hydrogen and CO, with the remaining balance of steam. To respect the assigned oxidiser composition and mass flow at cathode inlet, the resulting SOFC-2 air oxygen utilisation is close to 6%.

In this preliminary simulation, SOFC-2 voltage and power output is zero and the resulting thermal balance reflects heat

Table 3
Thermodynamic properties and chemical composition for the relevant points of cycle A (Figs. 4 and 5)

Points	G[a]	T (°C)	p (bar)	Molar composition (%)								LHV (MJ/kg)
				Ar	HC[b]	CO	CO_2	H_2	H_2O	N_2	O_2	
1	1.000	15.0	1.01	0.92	0.00	0.00	0.03	0.00	1.03	77.28	20.73	–
2	0.990	107.0	3.82	0.92	0.00	0.00	0.03	0.00	1.03	77.28	20.73	–
3	0.990	722.9	3.67	0.92	0.00	0.00	0.03	0.00	1.03	77.28	20.73	–
4	0.921	900.0	3.49	0.98	0.00	0.00	0.03	0.00	1.10	82.51	15.38	–
5	0.921	757.4	3.42	0.98	0.00	0.00	0.03	0.00	1.10	82.51	15.38	–
6	0.952	900.0	3.31	0.94	0.00	0.00	0.43	0.00	5.82	79.44	13.36	–
7	0.962	621.0	1.04	0.94	0.00	0.00	0.43	0.00	5.78	79.42	13.43	–
8	0.962	133.6	1.01	0.94	0.00	0.00	0.43	0.00	5.78	79.42	13.43	–
9	0.022	400.0	14.2	0.00	95.69	0.00	0.00	0.00	0.00	4.31	0.00	46.30
10	0.091	900.0	3.48	0.00	0.00	7.65	25.72	12.35	62.85	1.43	0.00	2.18
11	0.091	696.1	1.15	0.00	0.00	7.65	25.72	12.35	62.85	1.43	0.00	2.18
12	0.091	81.2	1.10	0.00	0.00	0.06	33.30	19.93	45.27	1.43	0.00	2.05
13	0.059	35.0	11.19	0.00	0.00	0.11	60.55	36.62	0.50	2.61	0.00	3.11
14	0.009	300.0	10.96	0.00	0.00	0.25	13.21	80.75	0.00	5.81	0.00	21.43
15	0.022	550.0	5.50	0.00	0.00	0.00	0.00	0.00	100.00	0.00	0.00	–
16	2.227	25.0	14.00	Selexol								–
17	0.051	25.0	120.00	0.00	0.00	0.00	100.00	0.00	0.00	0.00	0.00	–

[a] Mass flow rates are relative to the to the compressor inlet air flow (point 1, equal to 98.54 kg/s).
[b] Total hydrocarbons (see Table 9 in Appendix A).

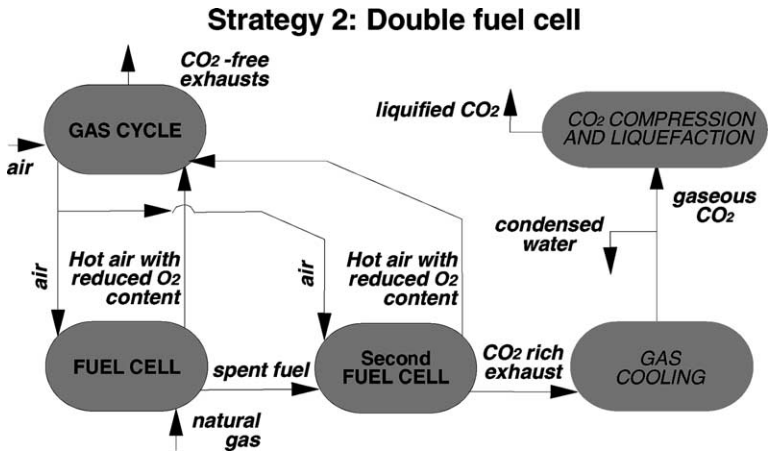

Fig. 6. Conceptual overview of the power cycles with double fuel cell.

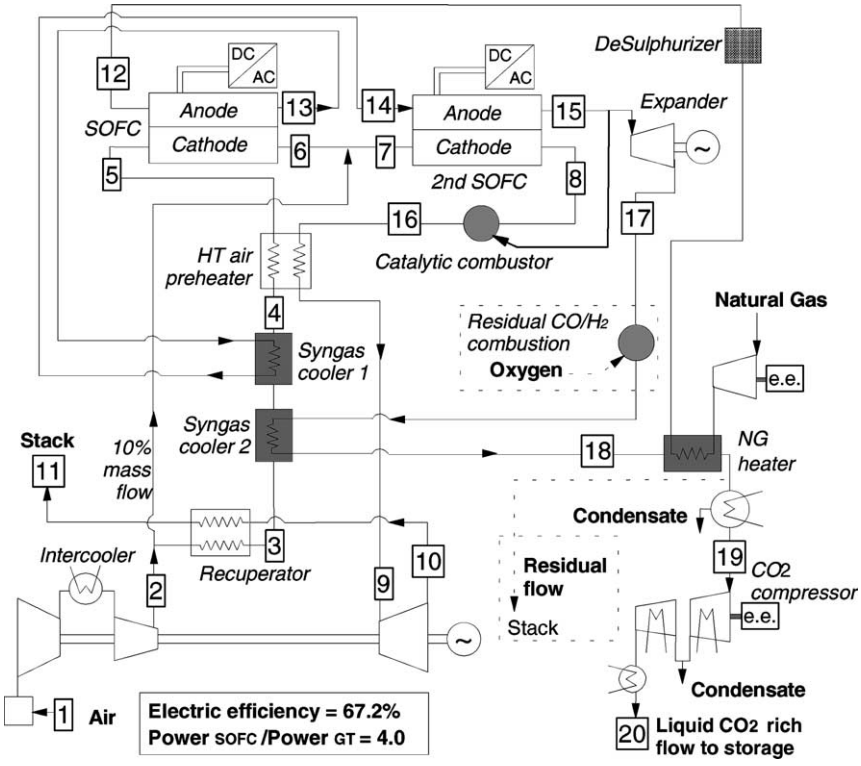

Fig. 7. Cycle configuration with double SOFC (dashed lines for option B only).

exchange to the anode/cathode flows of the entire oxidising reaction heat.

SOFC-2 anode exhaust gas is expanded down to ambient pressure, generating a relevant fraction of the plant power output. The gas expander works without cooling, with a maximum inlet temperature close to 930 °C. Two possible plant configuration options are then considered.

1) In the first case A, a 90% fraction of SOFC-2 anode outlet gas is expanded and cooled. After water condensation the remaining flow (#19A in Table 4, with 86.7% CO_2) is sent to the CO_2 compression/separation process, achieving 90% CO_2 sequestration. The residual 10% anode outlet flow (containing a $CO_2 + CO + H_2 + N_2$ mixture) is fed to a catalytic combustor which oxidises CO and H_2, with the resulting exhaust gas (#16) used for SOFC air preheating and expanded in the gas turbine cycle.
2) The second case B, addresses the alternative option of oxygen[1] combustion of the entire fuel cell anode

[1] Pure oxygen has been considered for simplicity. Combustion is placed downstream the turboexpander to reduce temperatures and avoid the requirement of blade cooling.

Table 4
Thermodynamic properties and chemical composition for the relevant points of the double-SOFC cycle of Fig. 7 (configuration without oxygen combustion, except for #19 and 20 which are given for cases A and B)

Point	G[a]	T (°C)	p (bar)	Molar composition (%)								LHV (MJ/kg)
				Ar	HC[b]	CO	CO_2	H_2	H_2O	N_2	O_2	
1	1.000	15.0	1.01	0.92	0.00	0.00	0.03	0.00	1.03	77.28	20.73	–
2	0.990	107.0	3.82	0.92	0.00	0.00	0.03	0.00	1.03	77.28	20.73	–
3	0.891	497.0	3.75	0.92	0.00	0.00	0.03	0.00	1.03	77.28	20.73	–
4	0.891	555.7	3.59	0.92	0.00	0.00	0.03	0.00	1.03	77.28	20.73	–
5	0.891	723.7	3.52	0.92	0.00	0.00	0.03	0.00	1.03	77.28	20.73	–
6	0.829	900.0	3.41	0.98	0.00	0.00	0.03	0.00	1.10	82.50	15.38	–
7	0.928	820.9	3.41	0.98	0.00	0.00	0.03	0.00	1.10	81.94	15.95	–
8	0.918	934.0	3.31	0.98	0.00	0.00	0.03	0.00	1.10	82.73	15.14	–
9	0.927	780.0	3.25	0.98	0.00	0.00	0.36	0.00	1.23	82.47	14.96	–
10	0.937	527.0	1.03	0.98	0.00	0.00	0.36	0.00	1.23	82.47	14.96	–
11	0.937	159.3	1.01	0.98	0.00	0.00	0.36	0.00	1.23	82.47	14.96	–
12	0.020	400.0	13.46	0.00	95.69	0.00	0.00	0.00	0.00	4.31	0.00	46.30
13	0.082	900.0	3.41	0.00	0.00	7.52	25.85	12.13	53.1	1.43	0.00	2.136
14	0.082	700.0	3.34	0.00	0.00	7.52	25.85	12.13	53.1	1.43	0.00	2.136
15	0.092	934.0	3.32	0.00	0.00	0.773	32.59	1.192	64.0	1.43	0.00	0.191
16	0.927	935.7	3.31	0.98	0.00	0.00	0.39	0.00	1.80	81.85	14.97	–
17	0.083	731.4	1.07	0.00	0.00	0.773	32.59	1.192	64.0	1.43	0.00	0.191
18	0.083	527.0	1.05	0.00	0.00	0.773	32.59	1.192	64.0	1.43	0.00	0.191
19A	0.048	30.0	1.01	0.00	0.00	2.05	86.71	3.17	4.25	3.81	0.00	0.191
19B	0.049	30.0	1.01	0.00	0.00	0.00	91.62	0.00	4.36	4.02	0.00	–
20A	0.047	25.0	120.0	0.00	0.00	2.14	90.57	3.31	0.00	3.98	0.00	0.195
20B	0.048	25.0	120.0	0.00	0.00	0.00	95.80	0.00	0.00	4.20	0.00	–

[a] Mass flow rates are relative to the to the compressor inlet air flow (point 1).
[b] Total hydrocarbons (see Table 9 in Appendix A). With respect to the plant configurations of Fig. 4, SOFC pressure losses have been reduced, as the stack no longer includes air preheating and combustion plenum, while SOFC-2 does not require fuel recirculation and pre-reformers.

exhaust. This arrangement allows to completely eliminate the residual CO and H_2 fraction (about 0.8 and 1.2%, respectively at point #16; the oxygen flow is stoichiometric) thus generating a $CO_2 + H_2O$ mixture with a small amount of nitrogen. The majority of steam is condensed before #19B in Table 4, giving a 91.6% rich CO_2 flow. Aiming to achieve the same level of CO_2 sequestration of the other cases, 90% of the gas mixture is sent to the CO_2 compression process for sequestration, while the remaining 10% is vented to stack (dashed lines in Fig. 7).

In both the cases, generation of a liquid, CO_2-rich flow from a gas mixture containing about 6% incondensable species (as N_2 and, if present, H_2 in flow #18) requires high pressure ratios[2] if a direct intercooled compression process is adopted. The electric power consumption of the gas mixture intercooled compressor becomes then comparable with the total electric consumption of the physical absorption + CO_2 liquefaction process considered for the first kind of power plants (with CO_2 separation train) considered in this paper. Moreover, traces of hydrogen and CO would dilute in case A in the final high pressure liquid CO_2 flow; problems may arise, depending on the storage technology, which are anyway not addressed here.

The comparison between the two cases (see also the final energy balances of Table 6) shows the following results.

1) The most significant difference is of course the requirement of a relevant oxygen flow (about 0.12 kg/s) in the second case, which adds complexity to the power plant. The additional energy consumption for the generation of oxygen would be close to 1000 kJ/kg O_2 (as by typical air separation units [24]).
2) In case A, the residual heating value carried by the unoxidised fraction of CO and H_2 at #17 is lost, while it is recovered by combustion in case B. The additional heat released at syngas cooler 2 in Fig. 7 yields a slightly higher optimum TIT and pressure ratio for the gas turbine cycle, generating 5% more power.
3) Both plants are calculated for a 90% CO_2 removal rate, aiming to compare their performance with the first plant (Fig. 5) presented in this paper. This figure could approach 100% by (case A) expanding the entire fuel flow, eliminating the catalytic combustion of the recirculated fraction or (case B) compressing all the expanded flow without venting a 10% fraction. The consumption of the CO_2 compressor will of course increase with the same proportion.

[2] Calculation with ASPEN® [20] yields a liquid mixture at 120 bar, 30 °C using Peng–Robinson equation of state for pure compounds with Wong–Sandler mixing rules (PRWS model). In the cycle of Fig. 5, pure CO_2 is already liquid at 80 bar, thus requiring a lower compression work.

4) The global performance of the two configurations gives 0.9% efficiency advantage to case B: the first case reaches 67.2% net LHV electrical efficiency versus 68.1% for the second case with oxygen combustion, including the consumption for oxygen generation.

The efficiency difference between the two cycles would become lower if a higher fuel utilisation for the second SOFC (90% in this simulation) should be assumed. The most interesting configuration is anyway probably the first, thanks to its relatively greater simplicity.

3.3.3. *Effect of SOFC-2 voltage*

As already mentioned, the role of the second SOFC in this power cycles is limited to the fuel oxidisation: cycle performances are calculated for the case of SOFC-2 generating zero-power ($V_c = 0$) and acting as a true "afterburner". Different cases have also been considered (based on case A in Fig. 7), where the power contribution and the cell voltage of the additional SOFC ranges from zero up to a maximum value of 0.5 V. The hypothesis of a voltage limit of 0.5 V has been set according to the cell voltage calculation discussed in Appendix A.2.2.

Fig. 8 shows the effect of a positive power contribution of SOFC-2 on the cycle efficiency: for a SOFC-2 cell voltage of 0.5 V the cycle efficiency could be increased of about 2.4% points. The double-SOFC cycle then becomes the most efficient in the comparison of Table 6. The efficiency gain is anyway close to 1.5% at an intermediate value of $V_c = 0.3$ V. When considering a cycle fuel input of 100 MW (Table 6), the SOFC-2 power output could reach a maximum of 6.2 MW at 0.5 V. The increased electric efficiency of the SOFC system yields a lower heat generation and progressively decreases the gas cycle optimum turbine inlet temperature and power output. For this reason the total cycle power output increase is limited to ≈2.4 MW at 0.5 V. The efficiency gain leaves of course unaffected the cycle CO_2 removal rate.

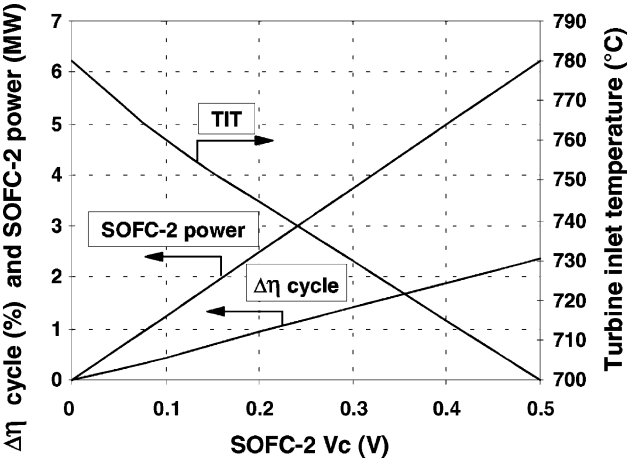

Fig. 8. Effect of the SOFC-2 voltage on the cycle performances.

4. Second law analysis and comparison of the SOFC cycle configurations

SOFC cycle configurations discussed above yield net electric efficiency ranging between 67.2 and 69.4%. Better thermodynamic understanding of these results can be obtained by a second law analysis, investigating cycles reversible work balances.

The comparison is homogeneous thanks to the coherence of the simulation assumptions and the use of the same calculation model.

The second law efficiency is defined as:

$$\eta_{II} = \frac{P_{el}}{W_{rev_f} m_f} \quad (5)$$

while the second law losses are defined as:

$$\Delta\eta_{II} = \frac{T_{amb}\Delta S}{W_{rev_f}} \quad (6)$$

Table 5 gives the various second law efficiency losses, grouped in the following terms:

- irreversibility occurring in the fuel cell (including power conditioning, heat exchange, heat losses, pressure drops, etc.) (1), and irreversibility occurring in the catalytic combustors (2);
- fluid-dynamic losses during air compression (3) and during gas turbine expansion (4);
- heat transfer, heat losses and pressure drops occurring in the recuperator and HT air heater (5) and in all other heat exchangers (6);
- losses for CO_2 separation, including shift process, CO_2 absorption, compression and liquefaction (7);
- all mechanical, electrical, auxiliary losses (including oxygen separation (8) and stack losses (9);
- loss for disposal of a high pressure, CO_2-rich liquid flow (10).

Comparison of second law efficiency losses suggests the following comments.

Table 5
Second law analysis of the considered SOFC cycles

Second law losses ($\Delta\eta_{II}$, %)	SOFC with CO_2 separation train	Double SOFC	
		A	B
(1) SOFC	11.69	14.84	14.83
(2) Combustor	5.53	0.46	0.40
(3) Air compressor	1.25	1.37	1.39
(4) Gas turbine	0.94	0.95	0.97
(5) Recuperator and HT air preheater	2.91	3.48	4.24
(6) Other heat exchangers	3.42	6.74	6.68
(7) CO_2 separation/compression	2.75	0.24	0.31
(8) Mechanical and auxiliary	0.76	0.64	0.81
(9) Stack	2.33	2.77	2.67
(10) Liquid CO_2-rich flow	1.07	3.35	1.51
Second law efficiency (η_{II})	67.35	65.16	66.19

1. The sum of FC and combustor loss is 1.9% larger for the first cycle, i.e. fuel oxidisation is performed with lower irreversibility by the double-SOFC cycle.
2. Compressor and turbine losses are practically constant, as the gas turbine cycle always operates under similar conditions.
3. The double-SOFC configuration suffers of a more complex heat exchanger network, leading to larger heat exchange losses (≈10 versus 6%).
4. The recuperator and HT preheater losses are higher for the double-SOFC cycle due to combined effects of higher gas temperature at SOFC-2 exit, higher heat exchange duty and lower pressure ratio.
5. CO_2 separation losses for the first cycle weight for ≈2.75 efficiency points (including shift, raw syngas compression, absorption process and CO_2 liquefaction), and for only ≈0.3 points in the double-SOFC configurations (intercooled compression of the syngas up to 120 bar). Double-SOFC cycle A suffers a high loss for the disposal of a liquid CO_2 flow with a residual heating value; as already mentioned, this loss could be reduced by increasing the SOFC-2 fuel utilisation.
6. The double-SOFC cycles show a slightly higher stack loss due to the relatively high temperature of its main exhaust stream (159 °C).

Globally the complexity of the CO_2 separation train of the first cycle, and its lower efficiency fuel oxidisation, are more than counterbalanced in the double-SOFC configurations by the necessity of a more complex heat exchanger network.

Table 6 reports the most relevant results for the energy balances of the considered plants.

The first cycle reaches the highest efficiency (69.3%), taking also advantage from a higher gas turbine output (23 versus ≈19% of the net output). The situation changes only if a substantial positive contribution from the second SOFC is assumed. Heat released to cooling fluids is comparable in the three cases.

As far as plant complexity is concerned, the first configuration suffers the presence of the shift reactors but, considered the high expected SOFC specific cost, this plant shows a more favourable SOFC/gas turbine power output ratio (3.3:1 versus 4:1). In all cases a 4–5% contribute to the

Table 6
Energy balances for the proposed SOFC cycles

Energy balance (MW)	SOFC with CO_2 separation train	Double SOFC (A)	Double SOFC (B, with O_2 combustion)
Natural gas input (LHV)	100.00	100.00	100.00
Electric power balance			
SOFC system output	53.8	53.72	53.76
Gas turbine cycle output	16.1	12.57	13.20
Syngas expander	3.13	3.03	3.35
Total produced power	73.03	69.32	70.31
Raw syngas compressor	1.70	–	–
Natural gas compressor	0.07	0.07	0.07
Absorption process consumption	0.44	–	–
Oxygen production plant	–	–	0.12
CO_2 compressor	1.48	2.07	1.99
Total absorbed power	3.69	2.14	2.18
Net power output	69.34	67.18	68.13
Net power output with SOFC-2 at 0.5 V	–	69.53	70.47
Heat released to cooling water			
Intercooler	5.01	5.51	5.51
Syngas cooling	16.1	13.63	15.96
Absorption process	0.18	–	–
CO_2 compressor coolers	2.41	3.32	3.34
Total heat released	23.7	22.46	24.81
Heat transferred in GT recuperator	50.94	40.1	42.0
Heat transferred in HT air preheater	15.15	18.5	14.6
Mass flow at air compressor inlet (kg/s)	98.54	108.5	108.5
CO_2 mass flow removed (kg/s)	5.0	5.0	5.0
CO_2 removal efficiency (%)	90.1	90.0	90.0
Specific CO_2 emission (kg/kWh_{el})	0.0288	0.0298	0.0294
Overall net efficiency (%)	69.34	67.18	68.13

produced power comes from the turboexpander which cools the depleted fuel at the cell exit.

It is interesting to note how the gas turbine size which would be required to build these power plant should feature an inlet air flow of 10–20 kg/s, which is typical for industrial units with 20–30 MW of nominal power output. The gas turbine power contribution is instead lower in these cycles, due to the low turbine inlet temperatures and pressure ratio and to the predominant role of the fuel cell.

Both plants achieve 90% or more of CO_2 removal. The double-SOFC configurations show the potential to achieve a 100% CO_2 removal rate thanks to high purity of the final anode exhaust gas (above 86.7% CO_2 versus 62.8% for the cases with a single SOFC) and to the eventual possibility of adopting a residual combustion with oxygen. The 90% CO_2 removal rate of the first kind of plant could be anyway enhanced with a more efficient absorption process without affecting plant thermodynamics.

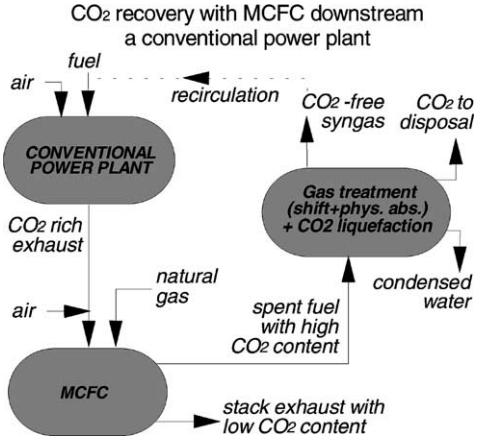

Fig. 9. Conceptual view of CO_2 separation from conventional power plant exhausts by use of a MCFC.

5. CO_2 separation from conventional power plants integrated with MCFCs

As discussed in Section 3.1, it is possible to imagine an exploitation of MCFC features by considering to place a MCFC system downstream a conventional ‘‘combustion fired’’ power plant, feeding the cathode with its exhaust gases with the aim of concentrating and then separating a fraction of the CO_2 otherwise vented. The possibility of ‘‘retrofitting’’ existing fossil-fuel power plants by extracting CO_2 from their stack exhausts is considered by the plant scheme of Fig. 9.

This configuration would give the possibility of separating the majority of CO_2 from the concentrated MCFC anode exhaust, leaving the remaining to the stack by the cell cathode exhaust. The basic condition for the feasibility of such a combination of technologies would be the presence of a reasonably high CO_2 fraction in the power plant exhaust gases, i.e. a 15–16% CO_2 content as typical for conventional pulverised coal steam plants with nearly stoichiometric air/fuel ratio. Such gas mixture shall be anyway mixed with air in order to add the amount of oxygen required for the formation of carbonate ions.

Let us consider an advanced coal steam cycle, a USC steam cycle. An example of this kind of power plant is represented by the two 400 MW ‘‘convoy’’ pulverised coal power plant of the Dutch electric utility ELSAM, featuring maximum steam pressures of 290 bar, double reheat and net electric efficiency close to 45% [25].

Table 7
Thermodynamic properties and chemical composition for the relevant points of the MCFC cycle shown in Fig. 10

Point	G[a]	T (°C)	p (bar)	Molar composition (%)[b]								LHV (MJ/kg)
				Ar	HC[c]	CO	CO_2	H_2	H_2O	N_2	O_2	
1	1.000	15.0	1.01	0.92	0.00	0.00	0.03	0.00	1.03	77.28	20.73	–
2	0.111	15.0	1.01									24.195
3	1.126	140.0	1.02	0.84	0.00	0.00	16.35	0.00	12.46	70.35	0.00	–
4	0.533	15.0	1.01	0.92	0.00	0.00	0.03	0.00	1.03	77.28	20.73	–
5	1.659	582.0	1.09	0.86	0.00	0.00	11.0	0.00	8.79	72.59	6.76	–
6	1.383	677.0	1.07	0.98	0.00	0.00	3.29	0.00	10.00	82.63	3.10	–
7	0.025	15.0	1.01	0.00	95.69	0.00	0.00	0.00	0.00	4.31	0.00	46.30
8	0.040	197.8	1.50	0.00	0.00	0.00	0.00	0.00	100.0	0.00	0.00	–
9	0.065	570.2	1.12	0.00	38.07	0.00	0.00	0.00	60.8	1.13	0.00	17.82
10	0.341	677.0	1.09	0.00	0.00	4.82	49.66	5.49	39.66	0.37	0.00	0.88
11	0.341	190.0	1.03	0.00	0.00	0.07	54.42	10.24	34.90	0.37	0.00	0.82
12	0.271	35.0	11.0	0.00	0.00	0.10	83.16	15.66	0.52	0.56	0.00	1.03
13	0.030	35.0	10.9	0.00	0.00	0.42	33.75	63.55	0.00	2.28	0.00	9.16
14	0.242	25.0	80.0	0.00	0.00	0.00	100.0	0.00	0.00	0.00	0.00	–

[a] Mass flow rates are relative to the steam cycle inlet air flow (point 1, equal to 338.6 kg/s).
[b] Coal (Illinois #6): C, 61.27 wt.%; H, 4.69 wt.%; O, 8.83 wt.%; N, 1.10 wt.%; S, 3.41 wt.%; moisture, 12.0 wt.%; sulphur, 8.7 wt.%.
[c] Total hydrocarbons (see Table 9 in Appendix A for natural gas composition).

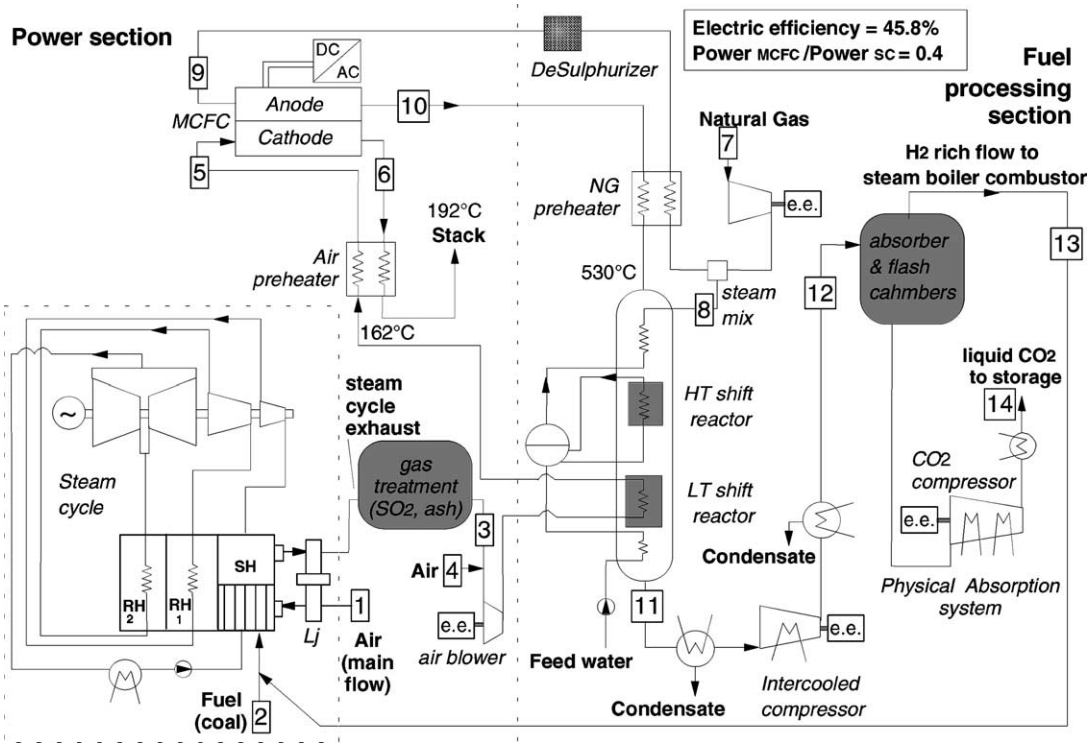

Fig. 10. CO_2 separation from a conventional power plant by integration with a MCFC plant.

Fig. 10 shows how the steam cycle could be integrated with a MCFC section, draining CO_2 from the steam cycle stack flow and concentrating the majority of CO_2 emissions in a lower mass flow rate stream (#10), not containing atmospheric nitrogen or excess oxygen. Table 7 lists the most relevant flow compositions; combustion in the steam cycle boiler has been considered for simplicity exactly stoichiometric. By the point of view of CO_2 separation, about 80% of the total carbon dioxide emission is contained by the MCFC anode exhaust (with a 49.6% molar concentration of CO_2, 71.4% mass at #10), leaving the remaining 20% in the very diluted (3.3 mol% CO_2 at #6) MCFC cathode exhaust.

CO_2 concentration in the MCFC anode exhaust gas is even higher than in the SOFC anode exhaust of Fig. 2. Such stream can be therefore sent to a fuel processing section as already considered by the chemical or physical absorption strategies of Fig. 5.

If a gas treatment similar to the one of Fig. 6 is adopted (including CO shift, raw syngas compression and 90% efficient CO_2 physical separation), the overall cycle net electric efficiency including MCFC output and gas treatment consumption slightly increases from the original 45% of the simple steam plant to 45.8% of the new plant, bringing about a substantial (40%) increase in the power output. Plant energy balance is presented in Table 8; for simplicity it has been considered that the original fuel input of the power plant were 1000 MW (LHV), so that the original electric power output was 450 MW_{el}.

With an addition of about 300 MW (LHV) natural gas input and with MCFC and CO_2 separation, the final power output becomes 595 MW. Due to the necessity of venting the diluted CO_2 contained in the cathode exhaust flow, the plant achieves a global CO_2 separation efficiency limited to 77%.

Table 8
Energy balance for the proposed MCFC cycle

Energy balance	Steam cycle + MCFC
Total fuel input (MW, LHV)	1299.5
Coal input (%, LHV)	70.1
Natural gas input (%, LHV)	29.9
MCFC system output (MW)	197.6
Steam cycle output (MW)	450.0
Total produced power (MW)	647.6
Air blower (MW)	5.44
Natural gas compressor (MW)	0.25
Raw syngas compressor (MW)	20.56
Absorption process consumption (MW)	2.92
CO_2 compressor	23.73
Total absorbed power (MW)	52.9
Net power output (MW)	594.7
Mass flow at air blower inlet (kg/s)	432.3
CO_2 mass flow removed (kg/s)	81.3
CO_2 removal efficiency (%)	76.9
Specific CO_2 emission (kg/kWh_{el})	0.148
Overall net efficiency (%)	45.77

It can be noticed that in the plant arrangement of Fig. 10, the hydrogen-rich flow resulting after CO_2 separation is sent to the steam plant boiler, thus decreasing of about 7% (LHV) the original fuel input. This solution has the advantages of easily solving the matter of inert species contained in this stream, which are simply mixed with the steam plant exhaust and vented after the MCFC at stack. A less simple alternative would be to separate this flow into two streams: the first always sent to the steam boiler, the second partially recirculated at the MCFC anode, balancing the increase of concentration of inert species in the gas treatment loop. This solution could yield a slight electric efficiency gain due to higher electric efficiency of the MCFC compared to the steam plant.

The assessment of the performances of such cycle has been made assuming that the lowest tolerable CO_2 fraction at the cathode inlet cannot fall much below 10% [26]. In order to match as closely as possible the MCFC plant operating conditions of Fig. 1, and with the aim of enhancing the CO_2 separation performances of the resulting cycle, an 11% CO_2 concentration at cathode inlet has been considered, resulting in the following MCFC parameters: 60% oxygen utilisation, 74% CO_2 utilisation, 80% fuel utilisation, cell voltage 0.7 V.

One of the most relevant difficulty in the MCFC application discussed here could arise from the necessity of adopting special care in cleaning the steam plant exhaust which would feed the MCFC. Exhaust gas treatment of the above-mentioned USC plant includes high-dust selective catalytic reduction (SCR, with NO_x emissions below 200 mg/Nm^3) and wet scrubber flue gas desulphurisation (FGD, with SO_2 emissions below 200 mg/Nm^3). A further very significant cleaning step would be necessary to achieve a dust (e.g. ashes) and sulphur content tolerable by the MCFC (e.g. sulphur components below 1 ppm [14]).

Those results are certainly much less attractive than those found for the SOFC plants of the previous paragraph, by the point of view of both lower efficiency and lower CO_2 separation rate; however, the above-discussed SOFC technology uneasily applies to fuels different from natural gas, and is not applicable to heavy fuels like coal unless more complex gasification technologies are considered. MCFC technology could instead have two advantages:

1) applicability to existing or advanced coal power stations, without the need of massive natural gas consumption (only 28% of the fuel input in Fig. 10 is natural gas);
2) fuel cell generation of ≈40% of the total plant power output, leaving the majority to lower capital cost components (steam cycle).

The proposed "CO_2-draining" MCFC technology instead uneasily applies to modern high efficiency natural gas combined cycle power plants, where the combustion products are substantially diluted with air to keep the gas turbine temperatures below materials limit, and the CO_2 fraction in the exhaust gas remains below 3–4% [27].

6. Conclusions

The intrinsic features of the electrochemical fuel oxidisation allow to easily applying the high temperature fuel cell technology to power plants projected for CO_2 separation.

The addition of a CO_2 separation train to the cell anode exhaust or the adoption of a double fuel cell configuration, when integrated with a proper gas turbine cycle, can lead SOFCs to achieve fuel-to-electricity conversion efficiency close to 70 with 90% CO_2 removal, with the further advantages of not requiring high turbine inlet temperatures and approaching zero-NO_x emissions. This efficiency level cannot be achieved with any other conventional technology.

Between the SOFC configurations proposed, the plant with unreacted fuel shift and physical absorption presents a higher efficiency; the double-SOFC configurations are advantaged by a simpler scheme and show best performances if the second "afterburner" SOFC yields a positive power output.

MCFCs could be successfully applied to carbon dioxide separation from conventional power plant exhausts. Despite the lower efficiency, the presented MCFC plant configuration has two important advantages in the possibility of exploiting coal as main fossil fuel and of substantially diluting the high costs of fuel cells with conventional power plant components.

High temperature fuel cells are presently under intense development by various manufacturers; production costs and demonstrated life still suggest that their application to medium or large scale power plants is probably confined in a medium-term perspective. However, the great potential of this technology in CO_2 emissions control may ensure to high temperature fuel cells a relevant role in the next future power generation.

Acknowledgements

The author wishes to thank Dr. Paolo Chiesa for his invaluable help and co-operation during the preparation of this paper and for his substantial contribution to modelling and simulation of the CO_2 absorption process.

Appendix A. Fuel cell models

A.1. Introduction

Table 9 summarises the most relevant assumptions which have been made for the simulations of the MCFC and SOFC cycles presented in this paper.

It shall be highlighted that the FC model adopted in this work is rather simplified if compared to more detailed models [28–30], which have been developed to trace cell internal temperature and flow composition distribution (with

Table 9
FC simulation assumptions

Fuel cell model assumptions	MCFC	SOFC
$\Delta p/p$ air side (%)	1	5
$\Delta p/p$ fuel side (%)	3	3
Heat loss (%)	1	1
Catalytic combustion efficiency (%)	99.5	99.5
Catalytic combustion ($\Delta p/p$) (%)	2	2
Fuel utilisation factor (global) (%)	78.5	85
Air utilisation factor (oxygen) (%)	55.6	30
Air utilisation factor (CO_2) (%)	76	–
Operating temperature (°C)	650	1000
Cell voltage (V)[a]	0.76	0.64
Oxygen-to-carbon ratio	1.5	2.0
Fuel pressure (bar)	1.013	1.013
LHV (kJ/kg)	46304	46304

Fuel (natural gas) composition: CH_4, 91.2%; C_2H_6, 4.4%; C_3H_8, 0.1%: N_2, 4.3%; sulphur compounds, 50 ppmv.
[a] $p = 1$ bar.

results strictly depending on a number of assumptions specific to a particular cell design).

Fuel cells are anyway operated here with inlet flow temperatures and compositions which are close to the nominal conditions used for model calibration. Both these conditions and the simulation assumptions of Table 9 are also usually considered "design" conditions, so that it is estimated here that the model adopted is adequate to the simulations performed (see also the comparison between the results of models with different level of detail discussed in [31]).

Exception may be constituted by the lower than usual cathode inlet concentration of: (1) CO_2 for the MCFC plant; and (2) O_2 for the second SOFC of Fig. 7, which also operates with high inlet temperatures; their effect is however easily accounted for, at least approximately, with the correlations for cathode composition proposed by [14] used in this work.

Other effects, such as the internal cooling balance of the second SOFC of Fig. 7, could be addressed with other models in a future work; calculation of heat balances for SOFCs is however performed here assuming a maximum gas outlet temperature limited to 900 °C, a figure which should prevent the formation of "hot spots" in the SOFC internal temperature distribution.

A.2. The SOFC calculation model

The SOFC model has been developed as a simplified and flexible tool for the simulation of a large variety of power cycle configurations. It simulates natural gas-fed tubular SOFC stacks with internal reforming, as schematically shown on the left side of Fig. 3. The model has been in particular calibrated on the performances of a 100 kW_{el} prototype plant [3,4,16], which has been working at atmospheric pressure and about 48% LHV electrical efficiency, running on natural gas (see the detailed discussion in [7]). The integration of the SOFC with gas turbine cycles requires the adjustment of some of the SOFC operating conditions (U_f, U_a, current density). Variation of reactant utilisation factors and cell current density influences also the cell voltage as discussed in Appendix A.2.2.

Based on the assignment of some input data including the fuel cell inlet flows compositions, fuel and air utilisation and average working temperature, the model calculates the thermodynamic properties and chemical composition of anode and cathode outlet flows, the fuel cell thermal balance (efficiency, heat generated) and second law analysis (entropy losses), the internal flow thermodynamic properties and compositions (modelling pre-reformed and reformed fuel composition, anodic recycling and residual flow combustion configurations) and FC operating parameters.

Some of the most distinctive features of the model are briefly summarised below.

A.2.1. Calculation of internal reforming

The requested fuel flow is calculated as a function of the assigned U_f and U_a ratios. For the case of SOFC-2 in Fig. 7, an assigned fuel flow and fuel utilisation results in a calculated air oxygen consumption and U_a.

Hydrocarbons are converted into a $H_2 + CO + CO_2 + H_2O$ mixture by steam reforming; the SOFC configuration considered here exploits steam contained in the partially recirculated anode exhaust gases. The recirculated fraction is calculated to match an assigned steam/carbon (S/C) ratio [13], depending on the C/H ratio of the fresh fuel.

Fuel recirculation is sustained inside the SOFC module by fresh-fuel-driven ejectors; the model calculates the requested inlet fuel pressure based on nozzle efficiency and momentum and mass balances. With natural gas feeding and a SOFC operating pressure of about 4 bar, the required fresh fuel pressure is in the range of 14–16 bar. A preliminary step of mixing and pre-reforming is calculated as an adiabatic process, with kinetic effects accounted for by an approach temperature difference with respect to thermodynamic equilibrium.

Fuel is then reformed inside the fuel cell, according to the steam reforming and CO-shift reactions already considered by Eqs. (2) and (3), where it is considered that the reforming reactions are completely developed thanks to the very high temperature conditions and to the catalytic effect of the anode materials. The CO-shift reaction is considered to reach thermodynamic equilibrium.

A.2.2. Cell voltage and efficiency

The model deliberately avoids a detailed analysis of the cell physical structure and the consequent introduction of a number of cell microscopic and geometrical parameters (components thickness, porosity, ohmic resistivity, etc.). A semiempirical cell voltage calculation is adopted, based on the data available in literature: calculation of cell voltage is performed as a function of the current density, of the operating temperature, of the operating pressure and of the reactant and products composition.

The primary influence of current density (i_c) on the SOFC performance (by ohmic, activation and concentration losses) is expressed by a reference set of $V_0(i)$ values, obtained by interpolation of available experimental data at standard operating conditions [14,15]. Calculation of the actual cell voltage value V_c is then performed by semiempirical logarithmic corrections derived by the Nernst potential equation accounting for the differences due to the real operating conditions (i.e. operating pressure, cathodic and anodic flow composition). The operating pressure effect is for instance expressed by:

$$\Delta V_p = 76 \log\left(\frac{p}{p_{ref}}\right) \quad (A.1)$$

For the application to the power cycles discussed in this paper, the calculated cell voltage at atmospheric pressure is 0.64 V at 300 mA/cm^2 with $U_a = 30\%$ and $U_f = 85\%$ ($U_f = 0.69$ for a single passage); the voltage rises up to 0.685 V at 4 bar.

The cell electrical efficiency $W_{el}/LHV_{fuel,in}$ is then a function of the cell voltage, of the fuel utilisation factor and of the inlet fuel composition, according to:

$$\eta_{el} = \frac{W_{el}}{LHV} = \frac{W_{el}/(nF)}{LHV/(nF)} = \frac{nFE}{LHV} = \frac{nFV_c U_f \Gamma_{H_2}}{LHV} \quad (A.2)$$

The quantity Γ_{H_2} is the fuel equivalent hydrogen content, expressed for a fuel mixture of $H_2 + CH_4 + CO + H_2O$ by the following equation [14]:

$$\Gamma_{H_2} = X_{H_2} + X_{CH_4} + X_{CO} \quad (A.3)$$

where X_{CH_4} and X_{CO} are the methane and carbon monoxide contribution to hydrogen formation, accounting for complete hydrocarbon reforming and CO-shift reaction.

Heat generated by irreversibility at the electrodes structure is given to the fuel and air flow, and partially lost by the stack external canister. A significant fraction of heat is consumed by the endothermic reforming reactions, thus reducing the requested cooling airflow and enhancing the fuel heating value.

The temperature increase of air and fuel flow across the fuel cell is calculated by an energy balance; calculation depends on air/fuel inlet temperature, air/fuel utilisation factors, cell voltage and efficiency, and accounts for the effects of fuel mixing and reforming.

A.3. The MCFC calculation model

The MCFC model has been developed based on the same principles of the SOFC model.

It requires the assignment of some input data including the fuel cell inlet flows compositions, fuel and air utilisation and average working temperature. As for the SOFC, the model calculates the thermodynamic properties and chemical composition of anode and cathode outlet flows, the fuel cell thermal balance (efficiency, heat generated) and second law analysis (entropy losses), and FC operating parameters, accounting for the internal reforming process of fuel hydrocarbons.

As shown in Fig. 1, the MCFC does not account on any internal recycling facility, and shall be fed with a steam + natural gas mixture at the anode (properly sustaining internal steam reforming, Eqs. (2) and (3)), as well as by an oxidant gas containing a correctly balanced proportion of $CO_2 + O_2$ at the cathode. Other details are substantially coherent with those discussed above for the SOFC model, with the exception of the calculation of the cell voltage, which has been substituted for simplicity by the assignment of the MCFC voltage, as by the simulation discussed in Section 2.2.

References

[1] W.L. Lundberg, S. Veyo, M. Moeckel, A high efficiency SOFC hybrid power system using the Mercury 50 ATS gas turbine, ASME paper 2001-GT-521, New Orleans, June 2001.
[2] M. Haines, Progress with the development of a CO_2 capturing solid oxide fuel cell, in: Proceedings of the 7th Grove Fuel Cell Symposium, London, September 2001.
[3] S. Veyo, The Westinghouse SOFC program—a status report, in: Proceedings of the 31st IECEC, no. 96570, 1996, pp. 1138.
[4] J. Sukkel, Two years experience with the 100 kW SOFC cogeneration unit at Arnhem, in: Proceedings of the 4th European SOFC Forum, Lucerne, Switzerland, July 2000, pp. 159–166.
[5] EPRI, 1993, TR-102931, Nth generation 2 MW Carbonate Fuel Cell Power Plant, Final Report, September 1993.
[6] M. Farooque, et al., Direct fuel cell development and demonstration activities at energy research corporation, in: Proceedings of the Fuel Cell Seminar, Palm Springs, 1998.
[7] S. Campanari, Thermodynamic model and parametric analysis of a tubular SOFC module, J. Power Sources 92 (2000) 26–34.
[8] S. Campanari, E. Macchi, The integration of atmospheric molten carbonate fuel cells with gas turbine and steam cycles, ASME paper 2001-GT-382, New Orleans, June 2001.
[9] S. Campanari, E. Macchi, Thermodynamic analysis of advanced power cycles based upon solid oxide fuel cells, gas turbines and Rankine bottoming cycles, ASME paper 98-GT-585, Stockholm, June 1998.
[10] S. Campanari, Full load and part-load performance prediction for integrated SOFC and microturbine systems, ASME J. Eng. Gas Turbines Power 122 (2000) 239–246.
[11] S. Veyo, L.A. Shockling, J.T. Dederer, J.E. Gillett, W.L. Lundberg, Tubular solid oxide fuel cell/gas turbine hybrid cycle power systems—status, ASME paper 2000-GT-550, June 2000.
[12] D.S. Vora, Southern California Edison 200 kWe pressurised SOFC power system, in: Proceedings of the 4th European SOFC Forum, Lucerne, Switzerland, July 2000, pp. 175–183.
[13] M. Mozaffarian, Solid oxide fuel cell for combined heat and power applications, in: Proceedings of the First European Solid Oxide Fuel Cell Forum, Lucerne, Switzerland, 1994.
[14] J.H. Hirschenhofer, D.B. Stauffer, R.R. Engleman, M.G. Klett, Fuel Cells Handbook, 4th ed., Parsons Co. for US Department of Energy (DOE), 1998.
[15] N.F. Bessette, R.A. George, Electrical performance of Westinghouse's AES solid oxide fuel cell, in: Proceedings of the 2nd International Fuel Cell Conference (IFCC 4–12), Japan, 1996.
[16] S. Veyo, W. Lundberg, Solid oxide fuel cell power system cycles, in: Proceedings of the International Gas Turbine and Aeroengine Congress and Exhibition, Indianapolis, June 1999, ASME paper 99-GT-356.

[17] M.R. Haines, W.K. Heidug, Demonstration of CO_2 capture from a solid oxide fuel cell, in: Proceedings of the Fourth European SOFC Forum, Lucerne, Switzerland, July 2000, pp. 365–374.
[18] P. Chiesa, S. Consonni, G. Lozza, A comparative analysis of IGCCs with CO_2 sequestration, in: Proceedings of 4th International Conference on Greenhouse Gas Control Technologies, Interlaken, Switzerland, 1998, pp. 107–112.
[19] G. Lozza, P. Chiesa, Natural gas decarbonization to reduce low CO_2 emission from combined cycles. Part A. Partial oxidation, Part B. Steam-methane reforming, Munich, June 2000, ASME papers 2000-GT-163/164.
[20] ASPEN PLUS, version 10.1, Aspen Technology Inc., Cambridge, USA, 1999.
[21] P. Chiesa, S. Consonni, Shift reactors and physical absorption for low-CO_2 emission IGCCs, J. Eng. Gas Turbines Power 121 (1999) 295–305.
[22] S. Campanari, P. Chiesa, Potential of solid oxide fuel cells (SOFC) based cycles in low-CO_2 emission power generation, in: Proceedings of the Fifth International Conference on Greenhouse Gas Control Technologies, GHGT-5, Australia, August 2000.
[23] C. Bagger, N. Christiansen, P. Hendriksen, E. Jensen, S. Larsen, M. Mogensen, Technical problems to be solved before the solid oxide fuel cell will be commercialized, in: Proceedings of the 1996 Fuel Cell Seminar, Courtesy Associates, November 1996, pp. 44–48.
[24] B.A. Hands, Cryogenic Engineering, Academic Press, London, 1986.
[25] H.J.R. Blum, Development of high-efficiency USC power plants in Denmark, in: Proceedings of the International Conference on Advanced Steam Plant, Institution of Mechanical Engineers, London, May 1997, no. 96570.
[26] P. Bedont, O. Grillo, A.F. Massardo, Off design performance analysis of a hybrid system based on an existing MCFC stack, ASME paper 2002-GT-301, Amsterdam, June 2002.
[27] G. Lozza, P. Chiesa, Natural gas decarbonization to reduce low CO_2 emission from combined cycles. Part A. Partial oxidation, Part B. Steam-methane reforming, ASME papers 2000-GT-163/164, 2000.
[28] E. Achenbach, Three-dimensional and time-dependent simulation of a planar solid oxide fuel cell stack, J. Power Sources 49 (1994) 333–348.
[29] J. Palsson, A. Selimovic, L. Sjunnesson, Combined solid oxide fuel cell and gas turbine systems for efficient power and heat generation, J. Power Sources 86 (2000).
[30] A. Selimovic, On design and off design performance prediction for a planar solid oxide fuel cell stack, in: Proceedings of the 4th European SOFC Forum, Lucerne, Switzerland, July 2000.
[31] L. Magistri, R. Bozzo, P. Costamagna, A.F. Massardo, Simplified versus detailed SOFC reactor models and influence on the simulation of the design point performance of hybrid systems, ASME paper 2002-GT-30653, 2002.